Assessment of building damage due to excavation-induced displacements: The GIBV method

Luca Piciullo[*], Stefan Ritter, Asgeir Olaf Kydland Lysdahl, Jenny Langford, Farrokh Nadim

Norwegian Geotechnical Institute, Sognsveien 72, 0806 Oslo, Norway

ABSTRACT

This paper presents an original methodology for the rapid assessment of "potential" building damage caused by an excavation. The combination of the Ground-work Impact (GI), in terms of induced greenfield displacements, and the Building Vulnerability (BV) form the basis for the GIBV damage assessment method. Both short- and long-term displacements are considered in the impact evaluation. In addition to short-term displacement due to undrained shear deformations, groundwater drawdown can result in significant consolidation settlements at considerable distance from the excavation site. In the proposed method for soft soil ground conditions, the short-term excavation-induced settlement is derived using empirical expressions and long-term displacement is estimated by coupling empirically-derived relationships for excavation-induced groundwater drawdown with a soil stratification model and consolidation theory. The building vulnerability is assessed by considering different physical characteristics and conditions of the buildings.

The GIBV method has been implemented in a GIS tool to predict damage classes for buildings exposed to excavation-induced settlements. Two different case studies in Norway were used to test the reliability of the predictions of the tool and validate the methodology. A comparison between the predicted damage classes with the back-calculated ones shows a relatively high accuracy of the methodology. Moreover, the coupled model, which considers both impact and vulnerability for the damage assessment of buildings, has a higher accuracy and lower overestimation rate compared to the results obtained by just considering the impact.

1. Introduction

Groundwork projects, such as deep excavations and tunnelling, are increasingly common in highly urbanized areas. Use of the underground is not limited to large-scale infrastructure projects (Broere, 2016). The displacements induced by groundwork projects can cause significant damage to adjacent buildings and assets. Protection of adjacent or overlying structures is a major part of the cost, schedule, and third-party impacts of urban underground construction (Son and Cording, 2005). An assessment of building damage nearby an excavation is an important step in identifying the most exposed structures to settlement-induced damage. Predicting and then, monitoring buildings belonging to a high class of damage is a key aspect in avoiding unexpected events and undesired costs. This prediction is complex and challenging due to several influencing factors, such as the ground conditions, the excavation and support system and characteristics of neighbouring buildings.

Different damage assessment approaches have been proposed in literature for the prediction of damage classes of buildings exposed to excavation-induced displacements. Son and Cording (2005), Aye et al. (2006), and Giardina et al. (2010), adopted a three-stage method, following the approach previously described by Mair et al. (1996). Stage 1 aims at identifying the buildings that can be potentially affected by displacements, based on the estimation of vertical and horizontal displacements from empirical relationships such as those proposed by Bowles (1988) and Clough and O'Rourke (1990). Usually, the maximum slope and maximum settlements for buildings are evaluated and compared with threshold values proposed by Rankin (1988). The buildings exceeding a given threshold are considered for Stage 2 analysis. In Stage 2, building strains, based on greenfield ground movement, are evaluated and related to limiting tensile strain values (Burland and Wroth, 1974; Burland, 1995; Boscardin and Cording, 1989). The buildings that are predicted to have an unacceptable damage level qualify for a more detailed evaluation including building characteristics and soil-structure interaction mechanisms (Stage 3). Each stage within this approach requires additional and more detailed information.

The approaches described above, and other similar approaches in

literature, mostly rely on the evaluation of the expected short-term impact, i.e. displacements or deformations of the greenfield concurrent to the excavation process. However, for soft soil conditions, pore pressure reduction due to groundworks can cause considerable settlements that develop with time (long-term impact). Neglecting these long-term effects can result in unconservative estimates.

Furthermore, most of the procedures available in literature neglect the building vulnerability in the damage assessment. Few studies considered vulnerability for the prediction of damage classes. Chiriotti et al. (2000), adjusted the damage classification according to Burland et al. (1977) by reducing the damage class values as a function of a vulnerability index. The vulnerability index is derived from an analysis of the information collected during the Building Condition Survey, BCS (Guglielmetti et al., 2008) using engineering judgment. The BCS consists of collecting information about the building history and in preparing a map of the building defects that (prior to construction) will be used to assess the vulnerability of the building (Guglielmetti et al., 2008). The higher the index, the greater is the reduction of the control parameter of each damage class defined in Burland et al. (1977). In this method, the vulnerability index is evaluated considering several structural, aesthetical and functional building characteristics. Unfortunately, not all these data are readily available for a preliminary analysis and the simultaneous assessment of several buildings can be time-consuming. Clarke and Laefer (2014) proposed a holistic approach to assess the building damage due to tunnelling works. The methodology assesses the buildings individually, according to both physical and cultural attributes. The damage assessment comprises two parts, damage and vulnerability predictions. The damage prediction employs traditional empirical and analytical methods to determine the degree of damage likely to be incurred. The vulnerability prediction is based on two criteria: community status and current condition (Clarke and Laefer, 2014). The community status is evaluated according to the historical significance and current use, following the work presented in Clarke and Hannigan (2009). The current condition is evaluated for each building by applying the University College Dublin Inspection Method (UCDIM). This methodology employs a damage assessment that is based strictly on the building's façade, and it is only suitable for brick-type buildings. The final damage class is obtained through a matrix correlating damage and vulnerability predictions. In this approach, vulnerability is conceived as potential adverse social consequences of damage to the building, reflecting the cultural aspects such as historical significance and current usage.

This paper presents a step forward into the - assessment of building damage due to groundwork-induced displacements. Specifically, this contribution aims to refine the stage 2 assessment described above by combining short- and long-term impact and vulnerability evaluations to derive building damage classes. The GIBV method is based on a soil stratification model, empirical observations of subsidence and ground water drawdown due to groundworks, short- and long-term displacements analysis and building vulnerability assessment. In the following sections the methodology and its implementation into an ArcGIS tool are described. The tool has been validated considering two case studies in Norway. The case study results are discussed and compared with real settlement measurements to demonstrate the reliability of the method in predicting building damage classes.

2. The assessment of building damage due to groundworks: The GIBV method

2.1. The concept behind the GIBV method

Ground-work Impact (GI), in terms of induced soil deformation, and the Building Vulnerability (BV) form the basis for the GIBV damage assessment method. The soil deformations, evaluated as greenfield displacements, are herein described as the sum of short- and long-term displacements. Short-term displacements are immediate displacements

that occur during the excavation due to shear deformations within the soil profile. These displacements are mainly a function of the depth of the excavation, type of retaining structure, type of soil, and distance from the groundwork location. Long-term displacements are the result of consolidation settlements due to pore water pressure reduction. The neighbouring buildings are exposed to the sum of the two effects. Often in literature, there is not an explicit distinction between the two different processes. One of the aims of this paper is to separately consider the two contributions and sum them together to define classes of impact for the buildings. The impact, herein, refers to the greenfield deformations due to groundworks. In a purely impact-based approach, those displacements are imposed at the base of the buildings assuming that the buildings are perfectly flexible. Vulnerability describes the building's predisposition to damage when it is subjected to ground deformations. In the approach proposed in this paper, vulnerability is evaluated considering physical building characteristics and the building condition. The combination of impact and vulnerability results in the expected building damage classes due to groundwork-induced displacements.

The concept behind the GIBV method is schematized in Fig. 1. All buildings not founded on bedrock are considered in the assessment process. The impact for these buildings is evaluated for both short- and long-term displacements. The values obtained are summed together and employed to assess the impact classes. The physical building characteristics and condition are then considered for the definition of vulnerability classes. Finally, the impact and vulnerability classes are combined in a matrix to differentiate among potential damage classes for buildings nearby groundworks. The GIBV method, presented in this paper, is suitable for identifying buildings susceptible of being damaged by groundwork and that require higher attention and detailed analyses.

2.2. Impact: Short-term displacements

In literature there are several empirical studies (e.g., Peck, 1969; Goldberg et al., 1976; Clough and O'Rourke, 1990; Bentler, 1998; Long, 2001; Moormann and Moormann, 2002; Konstantakos, 2008) and numerical simulations (e.g., Finno & Harahap, 1991; Ng, 1992; Whittle et al., 1993; Abdel-Rahman, 1993; Hashash & Whittle, 1996, 2002; Ng & Yan, 1999; El-Nahhas and Morsy, 2002; El-Sayed & Abdel-Rahman, 2002; Kung et al., 2007, 2009; Castaldo et al., 2013) dealing with the analysis of short-term excavation-induced displacements. These studies highlight that greenfield displacements are a function of different factors, namely type of soil, type of retaining structure, depth of the bedrock, excavation width and depth and factor of safety against basal heave.
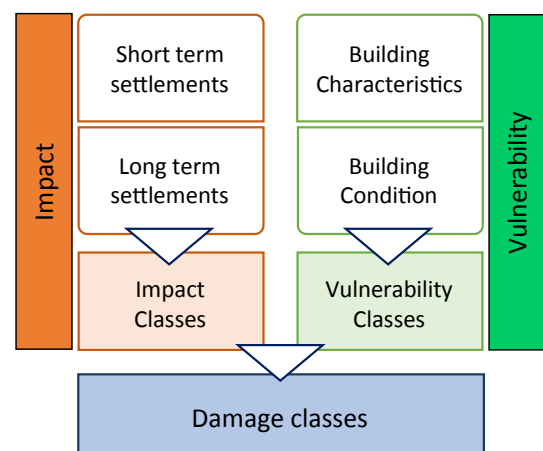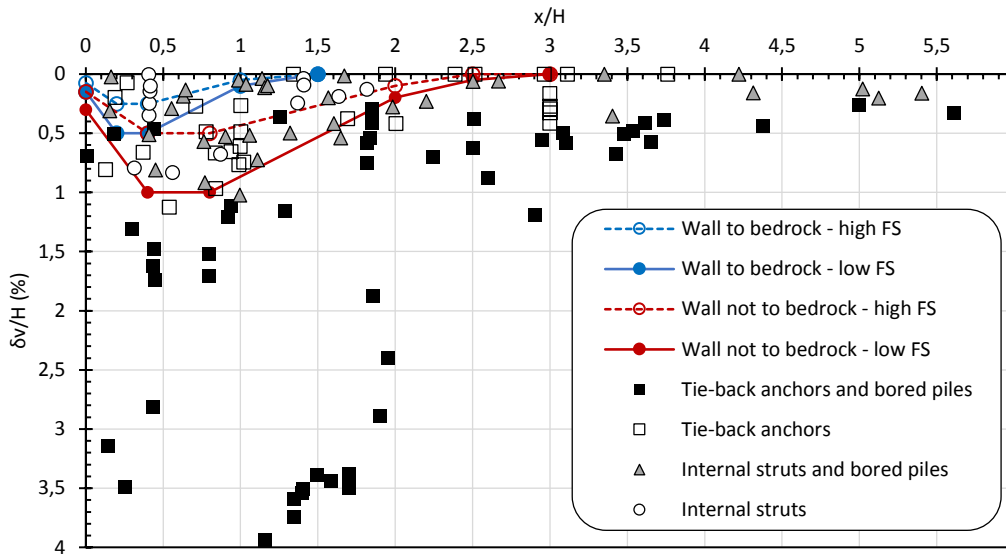

Fig. 1. GIBV concept.

Fig. 2. Expected normalized settlement, δv/H, versus normalized distance from wall, x/H in clay soils using different support methods. Black squares: drilled tie-back anchors and piles installed by drilling from the bottom of the excavation (e.g. steel core piles). White squares: Tie-back anchors. Grey triangles: internal strutting and drilled piles. White circles: internal struts. Red lines: expected settlements for wall not to bedrock for low (continuous line) and high (dotted line) factor of safety against bottom heave. Blue lines: expected settlements for wall not to bedrock for low (continuous line) and high (dotted line) factor of safety against bottom heave (modified from Langford et al., 2016). (For interpretation of the references to colour in this figure legend, the reader is referred to the web version of this article.)

Langford et al. (2016), presented curves that show the expected normalized vertical settlements (δv/H) and normalized distance from the wall (x/H) as a function of the factor of safety against basal heave. Fig. 2 compares these curves to field data. These curves have been defined combining modelling results from Karlsrud and Andresen (2005), and Mana and Clough (1981). In Langford et al. (2016), the variation away from the excavation, as initially suggested by Karlsrud (1997), was adjusted to better describe the empirical data for excavations with internal struts. The proposed curves (Fig. 2) can be grouped into wall to bedrock (blue curves) and floating wall (red curves). The continuous curves in Fig. 2 show the upper bounds for the two cases, considering a low safety factor against basal heave and/or stiff wall with relatively small distance between strut levels. The dashed curves represent the lower bounds for a high factor of safety, where a relatively flexible support wall and large distance between struts have been employed. The curves obtained have been compared with measured normalized settlements versus normalized distance for excavations in clay soils using different support methods (see Fig. 2, modified from Langford et al., 2016). The black squares represent projects where drilled tie-back anchors were used to support the wall, and piles were installed by drilling from the bottom of the excavation (e.g. steel core piles). The white squares are measurements of excavations supported with tie-back anchors. Projects involving internal strutting and drilled piles are marked with grey triangles. The white circles are representative of excavations with just internal struts. The combined installation of drilled tie-back anchors and bored piles inside an excavation (black squares), can lead to large ground settlements. The main causes are erosion, wash-out and disturbance from over-drilling and using flushing with large water or air pressure (Lande et al., 2020). In addition, drainage can cause pore pressure reduction at large distances (see Fig. 3), resulting in consolidation settlements far from the excavation (Langford and Baardvik, 2016). The comparison of the curves, with the measured settlements shown in Fig. 2, suggests that the continuous red curve can be adopted as a reasonable upper bound for an internally-braced excavation where no pore pressure reduction is expected (i.e. without drilling of piles or anchors and no leakage). Therefore, this curve was used for the evaluation of short-term displacements in the GIBV method. The curve represents the normalized vertical settlements as a function of the normalized distance from the wall in the case of an excavation with internal struts and sheet pile walls not installed to bedrock. It is important to mention that this is one of the several curves available in literature and that different ones can be employed in this methodology and implemented in the tool.
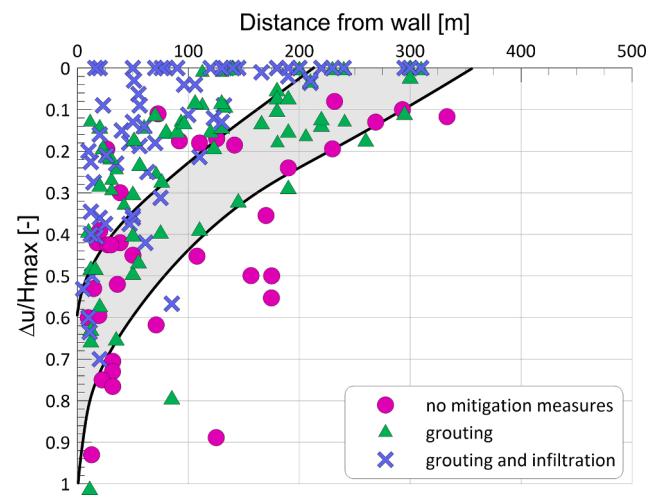

Fig. 3. Observed normalized decrease in pore pressure at base of clay layer as function of distance from the excavation based on case records from Norway (from Langford and Baardvik, 2016).

2.3. Impact: Long-term displacements

In addition to ground movements due to horizontal displacements of the supporting wall, displacements may also occur because of the increase of effective stresses due to pore water pressure reduction (e.g., Caspe, 1966; Goldberg et al., 1976; O'Rourke, 1981, 1993; Clough and O'Rourke, 1990; Ou et al., 1993, 2000; Hsieh and Ou, 1998; Poh et al., 2001; Kung, 2003). Leakage to the excavation can occur through the interface between the soil and the casings of tie-back anchors, the casings of tie-back anchors or piles, at the toe of the sheet pile wall or through uncovered bedrock. This leakage leads to the reduction of the pore water pressure in deeper permeable layers at the bedrock level, consequently leading to long-term settlements. The reason for the large pore pressure reduction and the large extension of the pressure draw-down can be mostly ascribed to the presence of permeable layers underlying non-permeable clay. Langford et al. (2015) and Langford and Baardvik (2016), examined the pore water pressure data from different deep excavation projects based on case records from Norway (Karlsrud, 1997; Braaten et al., 2004). While recognizing the existence of different

hydrogeological settings, construction methods and mitigation measures, some general trends can be observed by organizing the data according to the mitigation measures employed (Langford and Baardvik, 2016). Fig. 3 suggests that even for cases with grouting and infiltration, the maximum pore pressure reduction close to the excavation may reach up to 50% of the depth of the excavation below the groundwater level (H_{max}). In absence of mitigation measures, this value can reach up to 100% of H_{max}. Furthermore, such a reduction can extend as far as 350 m away from the excavation.

The GIBV method implements the upper and lower bound curves shown in Fig. 3. The lower bound curve is representative of the use of measures, including both grouting and infiltration wells, to limit the pore water pressure reduction. The upper bound curve represents the case of no mitigation measures. The curves show the maximum expected reduction of pore water pressure as a function of the excavation depth below the groundwater level (H_{max}) and the distance from the excavation.

To evaluate the settlements due to pore water pressure reduction, Janbu's modulus concept was used (Janbu, 1970). This method is largely used in Nordic countries (Andresen and Jostad, 2004) to calculate consolidation settlements. The tangent modulus M, or oedometer modulus, is a measure of the resistance against deformation (Janbu, 1970). The settlement calculation considers purely vertical stress and strain and the oedometer modulus M is expressed as:

$$M = \frac{d\sigma'_v}{d\varepsilon_v} \tag{1}$$

for overconsolidated (OC) soils

$$M = M^{OC} \quad \text{for } \sigma'_{v0} + \Delta\sigma'_v < \sigma'_{vc}$$

for normally consolidated (NC) soils

$$M = m(\sigma'_{v0} + \Delta\sigma'_v - p_r) \quad \text{for } \sigma'_{v0} + \Delta\sigma'_v > \sigma'_{vc}$$

where σ'_v and ε_v are, respectively, the vertical effective stress and vertical strain, σ'_{v0} is the initial vertical effective stress, p_r is the reference vertical stress for M = 0, and σ'_{vc} is the vertical preconsolidation stress. Assuming an increment of the initial vertical effective stress, σ'_{v0}, of a value $\Delta\sigma'_v$, the vertical strain increment is equal to:

$$\Delta\varepsilon_v = \int_{\sigma'_{v0}}^{\sigma'_{v0}+\Delta\sigma'_v} \frac{1}{M} d\sigma'_v \tag{2}$$

so that:

$$\Delta\varepsilon_v = \frac{\Delta\sigma'_v}{M^{OC}} \quad \text{for } \sigma'_{v0} + \Delta\sigma'_v < \sigma'_{vc}$$

$$\Delta\varepsilon_v = \frac{\sigma'_{vc} - \sigma'_{v0}}{M^{OC}} + \frac{1}{M} ln\left(\frac{\sigma'_{v0} + \Delta\sigma'_v - p_r}{\sigma'_{vc} - p_r}\right) \quad \text{for } \sigma'_{v0} + \Delta\sigma'_v > \sigma'_{vc}$$

The previous equations show how to calculate the vertical settlements due to given increase of vertical effective stress. The increase of the vertical effective stresses is a result of the reduction of pore water

pressure at the end of the consolidation phase.

2.4. Vulnerability

The methodology developed for the assessment of building vulnerability to groundwork-induced displacements is based on a combination of approaches available in literature for assessment of mining, tunnelling and seismic risk. The rating method (or point scoring system) for the assessment of the vulnerability class of a building in mining areas has been developed in USA (Bhattacharya and Singh, 1984; Yu et al., 1988) and Poland (Dzegniuk et al., 1997). This method considers several parameters to define the vulnerability class, such as building length, shape, type of foundation (Saeidi et al., 2012). The method is qualitative and consists of assigning a score to each parameter. The sum of all scores for each building is then compared with the ranges for five classes of vulnerability, resulting in the vulnerability class of that building.

Giardina et al. (2009) developed an assessment procedure for excavations based on the same principles of the Vulnerability Index Method used for seismic risk assessment (GNDT, 1993; Grünthal, 1998). It proposed a preliminary list of structural and non-structural characteristics influencing the building vulnerability due to groundworks-induced deformations, namely structural type, material quality, location (pure sagging, pure hogging, mixed profile), geometry, foundation type and existent damage.

Chiriotti et al. (2000) and Chiriotti and Grasso (2001), introduced the evaluation of a Vulnerability Index (Iv) to consider the different characteristics of the buildings and their susceptibility to damage due to tunnelling. The information for the index evaluation are gathered during the Building Condition Survey (BCS). This a priori survey (before the groundwork execution) aims at recording conditions and characteristics of buildings within a control zone. The building characteristics are grouped into different categories: structural, orientation and position, functional behaviour, aesthetic quality, and defect characteristics; which are the main indicators influencing the sensitivity of the building towards deformations (Chiriotti et al., 2000; Chiriotti and Grasso, 2001). As for the rating method, a value is assigned to each building characteristic. The sum of all values represents the building vulnerability index. The index is, then, classified into 5 categories of different degrees of severity as a function of its value. The same approach can be found in different publications dealing not only with groundworks (Giardina et al., 2012), but also with seismic risk assessments (Vicente et al., 2011; Ferreira et al., 2013, Ferreira et al., 2014; Maio et al., 2016).

In the GIBV method, to assign a vulnerability class to a given building, a Vulnerability Index (I_v) was defined following the procedure of Chiriotti et al. (2000) and Chiriotti and Grasso (2001), but using a reduced number of parameters for the index evaluation. The selection of parameters was carried out with respect to data availability and considering the approaches of Dzegniuk et al. (1997) and Giardina et al. (2012) and the BCS. The chosen parameters can be easily retrieved from GIS shapefiles and municipality digital archives. They represent building characteristics influencing the damage susceptibility due to groundworks and were grouped into three different categories (Table 1):

Table 1

Vulnerability classes for a building, based on a common evaluation of five attributes. Rating method adapted from Dzegniuk et al. (1997). The score for each class is shown in square brackets.

Characteristic	Parameter	Class vi				Weight Pi	Max value	Relative weight
		A [0]	B [5]	C [20]	D [50]			
Geometrical	Building length (m)	≤10	11–15	16–30	>30	0.75	37.5	30%
	Building shape[1]	>0.75	0.75–0.5	0.5–0.35	<0.35	0.75	37.5	
Structural	Structure type	Steel	Reinforced concrete	Wooden, Mixed	Masonry, special structure	1	50	50%
	Foundation type	To bedrock, Piles	Raft	Strip	Wooden piles, isolated	1.5	75	
Condition	Visual damage	Excellent	Good	Medium	Bad	1	50	20%

[1] See Section 3.3.

geometrical characteristics, structural characteristics, and condition of the building. Each category is assessed by vulnerability parameters: building length and shape for the geometrical characteristics; type of structure and foundation for the structural characteristics; and visible damages for the current condition of the building. For each vulnerability parameter, four classes (C_{vi}) with different scores were defined: A[0], B [5], C[20], and D[50] (Table 1). The overall vulnerability is calculated as a weighted sum of the six parameters. A weight (p_i) is assigned to each parameter, ranging from 0.75, for the less important parameters up to 1.5 for the most important (see Table 1). A higher weight was assigned to the foundation type because it was judged to be more important than other parameters. Each building undergoes this procedure and a total vulnerability score (I_v*) is evaluated (Eq. (3)). This value is, then, normalized (I_v) (Eq. (4)) and used to assign a final vulnerability class to the building. The normalization coefficient used, is evaluated as the sum of the maximum values available for each parameter. The vulnerability index obtained ranges between 0 and 100 (Table 2).

$$I_v^* = \sum_{i=1}^{n} (C_{vi}{}^* p_i) \tag{3}$$

$$I_v = \frac{I_v^*}{\sum_{i=1}^{n} (C_{vD}{}^* p_i)} \tag{4}$$

n = number of parameters; C_{vD} = value of the maximum vulnerability class (D), i.e. equal to 50 (see Table 1).

The relative weight of each category in the calculation of the vulnerability index, is respectively 30, 50 and 20 percent for geometrical characteristics, structural characteristics, and building condition. It is important to underline that the weights can be changed as a function of the database at hand. Different values for the weights produce different relative weight of the three categories. The reliability of the proposed method increases as more information become available on the characteristics of the buildings and their condition. If the information on one or more vulnerability parameters is missing, then the highest class (C_{vi}) is considered in the calculation.

3. Implementation of the GIBV method in an ArcGIS tool

3.1. The aim of the tool

The GIBV method described in Section 2 has been implemented in an ArcGIS tool. The aim is to provide a practical tool for rapid and early-stage analysis of buildings exposed to damage from groundwork-induced displacements. The tool is programmed in Python and is directly accessible from the interface of the commercial software ArcGIS Pro Advanced and Standard. The required inputs necessary for running the short-term impact analysis are:

- shapefile polygon with the location of the excavation;
- shapefile polygon containing all buildings to be investigated;
- depth of the excavation (m).

The building and excavation feature classes must be in the same projected coordinate system. If the user enables the option "Long term settlement calculation", then few additional inputs are needed:

- raster showing depth to bedrock in metres;
- geotechnical characteristics of the main soft soil layer: thickness of dry crust (m), depth to groundwater table (m), total unit weight of soil (kN/m^3), overconsolidation ratio (-), pore water pressure reduction nearby the excavation (kPa), Janbu reference vertical stress, p_r (kPa), Janbu m value.

The "Vulnerability analysis" option is also available. To run this option, the user needs to specify the columns of the building feature class that contain vulnerability information. If the user does not specify any column for one or more vulnerability parameters (see Table 1), then those parameters are simply omitted from the index evaluation. Values/characteristics in the GIS shapefile attribute table must be specified for each vulnerability parameter. If the value is not part of the domain, the default value (maximum vulnerability class) will be assigned.

Once all the inputs are inserted, the tool can be run. The ArcGIS tool

Table 2
Vulnerability classes defined according to the normalised vulnerability index value.

	Vulnerability classes			
	Negligible	Low	Medium	High
Iv	0–25	25–50	50–75	75–100

Table 3
The maximum slope and the maximum settlement are categorized in four level of impact (Adapted from Rankin, 1988).

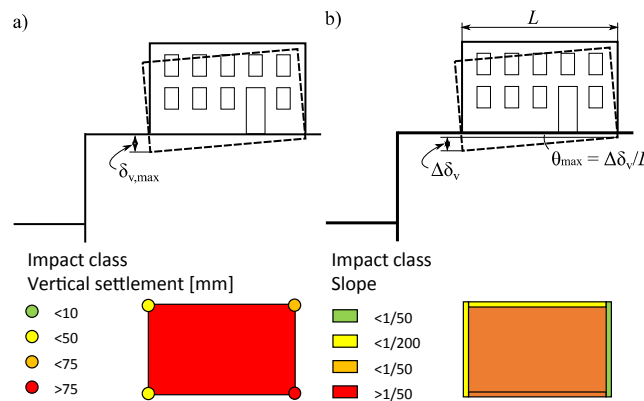| Impact level	Maximum rotation (θ_{max})	Maximum settlement ($\delta_{v,max}$)
1. Negligible	<1/500	<10 mm
2. Slight	1/500–1/200	10–50 mm
3. Moderate	1/200–1/50	50–75 mm
4. High	>1/500	>75 mm

Fig. 4. Building deformation parameters adopted for impact assessment: (a) maximum building settlement and (b) building slope. Examples of impact class definition as a function of: (a) the maximum vertical settlement of the building corner points; (b) the max slope of building walls.

Fig. 5. Expected damage classes and classification of the matrix cells. The 4 × 4 matrix plots the vulnerability against the impact classes.

produces a shapefile with the maximum vertical settlement ($\delta_{v,max}$) and maximum wall slope (θ_{max}) for each building. The shapefile contains the values for the short-and long-term displacements separately. The buildings are classified into four impact classes, according to the highest calculated displacements, and four vulnerability classes. The impact and vulnerability classes are finally combined in a matrix to obtain the expected damage class (see Fig. 1) for a given building.

3.2. Evaluation of short-and long-term impact on buildings

To evaluate the short-term displacements the curve correlating the normalized vertical settlements and the normalized distance from the excavation (Fig. 2) was implemented into the tool. This curve is representative of an internally braced excavation with a low stiffness wall and a low factor of safety, not affected by pore pressure reduction at the bedrock level. Knowing the distance of a corner point from the excavation makes it possible to estimate the expected vertical displacement (greenfield condition) of that point. For the long-term analysis, the GIBV method assumes a 2-layer soil, consisting of a dry crust (thickness specified by user) and, then, a deformable soil down to the bedrock. The depth to bedrock is specified by the bedrock model/sediment thickness raster. The soil layer is subdivided into slices of 1 m thickness and long-term consolidation settlement is evaluated for each of them. The evaluation of the expected vertical settlement is computed starting from the expected pore water pressure reduction. The user may choose between two different pore water reduction curves (see Section 2.3): lower bound and upper bound. These curves correlate the reduction of the pore water pressure with the distance from the excavation. In the calculations, it is assumed that the increase in the vertical effective stress is equal to the pore water pressure reduction ($\Delta u = \Delta\sigma'_v$, i.e., end of the consolidation

phase). Knowing the increment of the vertical effective stress, the vertical strain increment is evaluated by applying Janbu's method (Section 2.3). Finally, to evaluate the impact due to the excavation, the short-and long-term settlements are added up.

The buildings are schematized into corner points and line walls. The impact of the excavation is evaluated according to the location of the corner points. The vertical settlement (δ_v) and the slope (θ) are calculated respectively for every corner point and wall line (connecting two corner points), for both short- and long-term settlements. These deformation parameters are then classified according to the four categories proposed by Rankin (1988), in the so-called impact classes (Table 3). Each building can be classified either on the basis of the maximum vertical settlement ($\delta_{v,max}$) experienced by its corner points or on the basis of the maximum slope or rotation (θ_{max}) of the line walls.

An example of this application is shown in Fig. 4. The same building could have a different impact class as a function of the deformation parameter chosen for the classification. Usually, the vertical settlement is a more conservative approach than the slope.

3.3. Evaluation of building vulnerability

The buildings vulnerability is estimated using the method described in Section 2.4. Different building characteristics (see Table 1) are considered to define a vulnerability index. Calculation of the geometric characteristics of the buildings (length and shape) is done automatically in the GIS environment. The information concerning the structure type, building foundation and technical condition of the buildings should be provided by the user. Often this information is available in the building database(s) maintained by the municipality. The building characteristics are evaluated in the ArcGIS tool, as follows:

- length: building length in the direction of the construction, i.e., the difference between the greatest and shortest perpendicular distance from any corner to the excavation;
- shape: is a number representing the geometric squareness or complexity of a building polygon. It is evaluated considering the "isosquarimetric" version of the Polsby-Popper score (Polsby and Popper, 1991). It is the ratio of the building area to the area of a square evaluated as a function of its perimeter (Eq. (5)). If the result is 1, the building is a square. If the building cross section is irregular,

Table 4
The differential settlement values and the associated damage classes.

P[D ≥ Di|≥δρ]	Differential settlement [mm]	Defined damage classes
Up to 80% of D1 or higher	≤ 20	D0/D1
Up to 80% of D2 or higher	>20 and ≤60	D2
Up to 80% of D3 or higher	>60 and ≤100	D3
>80% of D3 or higher	>100	D4/D5

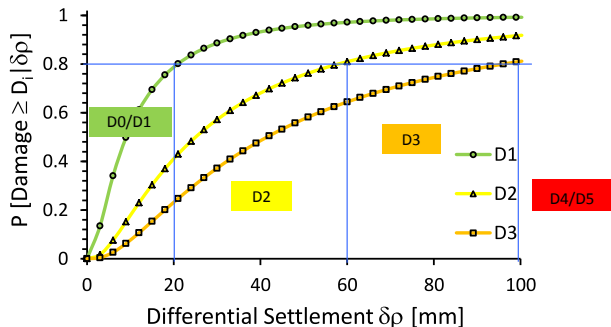**Fig. 6.** Fragility curve from Peduto et al. (2019). Threshold at 80% P and definition of different damage classes.

Fig. 7. Contingency matrix with the back-calculated damage classes as columns and the predicted ones as rows. The matrix cells are classified in correct prediction (CP), overestimation (O), underestimation (U), error (E). The sum of all the cells return the total number of buildings under investigation.

Table 5
Name and formula of the performance indicators considered.

	Formula
Accuracy	$\sum CP / \sum_{i,j=1}^{4} cells, ij$
Overestimation rate	$\sum O / \sum_{i,j=1}^{4} cells, ij$
Error rate	$\sum E / \sum_{i,j=1}^{4} cells, ij$
Underestimation	$\sum U / \sum_{i,j=1}^{4} cells, ij$

the result is less than 1. If the building is very elongated, the result is much less than 1.

$$\text{isosquarimetric} = 16 \frac{A}{P^2} \tag{5}$$

A = area of the building
P = perimeter of the building
- structure type, foundation type, visual damages depend on the values assigned by the user in the attribute table

If some of the above parameters are not specified, they are omitted from the calculation of the vulnerability index. The vulnerability classes (C_i) defined for each parameter are combined to evaluate the vulnerability index considering Eqs. (3) and (4). The vulnerability index is assigned to every building, and the data is automatically added to the ArcGIS project and symbolized.

3.4. Prediction of damage classes for buildings

After the vulnerability and impact classes have been defined, a matrix is used to evaluate the damage class for each building. The 4 × 4 matrix plots the four vulnerability classes against the four impact classes. Different matrix combinations and number of damage classes can be defined. The matrix configuration depends on the willingness to take risk which will often depend on the severity of the potential consequences. Thus, the distribution of the damage classes within the matrix can vary as a function of the project under investigation. The matrix proposed in this paper has five damage classes and a "stair" classification (Fig. 5). The classification used corresponds to the one used by several authors to classify visible damages of buildings (e.g. Jennings and Kerrich, 1962; MacLeod and Littlejohn, 1974; National Coal Board, 1975; Burland et al., 1977; Boscardin and Cording, 1989): D0-negligible (green), D1-very slight (light green), D2-slight (yellow), D3-moderate (amber), D4/D5-severe and very severe (red).

4. Validation of the GIBV damage assessment method: Comparison between predicted and back-calculated damage classes

4.1. Application of the tool and definition of back-calculated damage classes

The GIS tool was applied to two case studies in Norway with different urban contexts: Jong-Asker, Sandvika and Kredittkassen, Oslo. The first case study examines typical Norwegian wooden houses with shallow foundations nearby an excavation west of the town Sandvika. The houses range from one to three stories, but they are mostly two-storey buildings. The second case study is in the Oslo city centre. This excavation was surrounded by several urban buildings with different geometries and structure types. Settlement measurements are available for both case studies. The aim of the case studies was to test the reliability of the ArcGIS tool, apply the GIBV method to two different urban contexts, and validate/evaluate the results by comparing the predicted and measured damage classes.

The shapefiles necessary to run the analyses are houses and excavation polygons. Moreover, a raster reproducing the depth to bedrock is
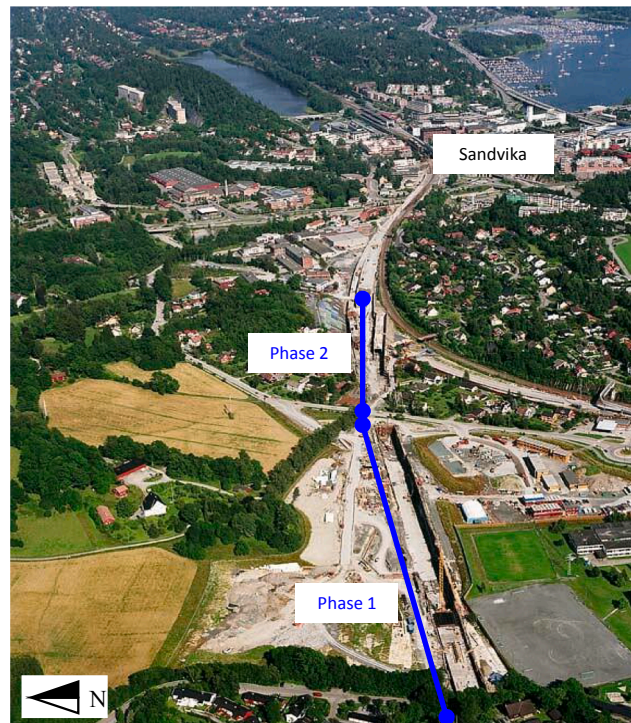

Fig. 8. Phase 1 and Phase 2 location of the Jong-Asker excavation.

Table 6

The input parameters for Jong-Asker and Kredittkassen case studies.

Variable	Unit	Jong-Asker	Kredittkassen
Depth of excavation	[m]	17	16
Dry crust thickness	[m]	1	3
Groundwater depth	[m]	2	2
Soil unit weight	[kN/m^3]	18.5	19
Overconsolidated ratio	[-]	1.1	1
Janbu's modulus number	[-]	19	19
Pore water pressure reduction at the bedrock	[kPa]	105	98

needed to evaluate the long-term settlements. The raster for Jong-Asker case study was established based on total soundings available in the area. About 360 geotechnical drillings were used to construct the bedrock model for the Jong-Asker case study. The drillings were located mostly along the railway corridor or at especially deep sediment basins.

The distance between the boreholes varied from 10 to 200 m. The depth to bedrock values (clay thickness) were interpolated using Kriging with variable search radius and zero nugget. The semivariogram range was set to 200 m to match the borehole data. The final bedrock raster was produced with 1×1 m cell size to match the scale of the buildings. To avoid unrealistic rotation values for short wall segments, the raster was then smoothed using the Focal Statistics GIS tool, averaging three cells in two directions. The depth values were interpolated, and the bedrock elevation was later calculated by subtracting the depth map from the terrain topography. The depth to bedrock model for Kredittkassen was provided by Oslo municipality (Eriksson et al., 2014). It is based on all reported drillings since the end of the 19th century until today.

To validate the predicted damage classes, the fragility curves for settlement-affected masonry buildings, developed by Peduto et al. (2019), were used to back-calculate damage classes based on measured settlement data for the two case studies. According to Peduto et al. (2019), the differential settlement of buildings, which was defined as the difference between the maximum and minimum settlements along sections of interpolated Interferometric synthetic aperture radar (InSAR)
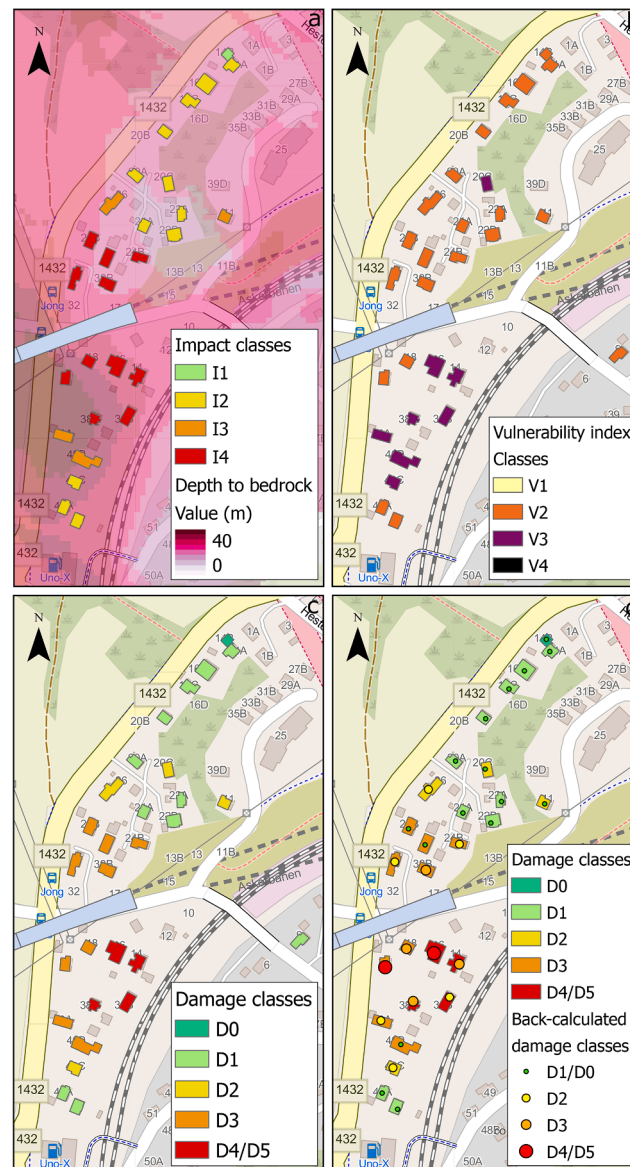

Fig. 9. Maps obtained applying the tool to the Jong-Asker case study: a. Impact classes; b. Vulnerability classes c. Damage classes; d. Comparison between predicted damage classes and back-calculated ones (dots).

derived settlement data, is the best subsidence-related metric that can be correlated to damage classes. For the case studies, the differential settlement of each building has been defined as the difference between the maximum and minimum measured settlements. Although this definition of differential displacements is slightly different compared to the one used in Peduto et al. (2019), this solution was the most feasible and applicable to obtain an indirect estimation of the damage classes for buildings. A log-normal distribution function is assumed to relate differential settlements with damage severity levels in the form of empirical fragility curves. For our purposes, the probability of having 80% of a given damage class was defined as threshold (see Fig. 6). Table 4 provides the differential settlement values and the associated damage classes.

To quantify the tool performance of correctly predicting the building damage classes a matrix (i.e., contingency table) of predicted versus back-calculated damage classes and a set of indicators were considered (Calvello and Piciullo, 2016; Piciullo et al., 2020). This approach stems from the contingency table analysis (Gokhale and Kullback, 1978; Jollife and Stephenson, 2003). The 4 × 4 matrix has the measured damage classes as columns and the back-calculated ones as rows (Fig. 7). The matrix cells are classified in correct prediction (CP), overestimation (O), underestimation (U) and error (E). The cells along the matrix principal diagonal are considered correct predictions. An exceedance of 1 damage class between predicted and back-calculated is also considered to be a correct prediction (CP). More than 2 damage classes difference between the prediction and the back-calculation is considered an overestimation (O). The underestimations are considered errors (E) if there is more than 1 class difference between back-calculated and predicted classes; otherwise they are underestimations (U). The cells are filled with the number of buildings belonging to a given combination of predicted and back-calculated damage classes (d_{ij}). The indicators used to quantify the matrix are also derived from contingency table analyses. The formulas and names are provided in Table 5.

4.2. Project description: Jong-Asker

The Norwegian National Rail Administration, Bane NOR (previously Jernbaneverket) built a double rail track between Sandvika and Asker during the period 2000–2004. The new double track branches off from the old railway line west of Sandvika (Fig. 8). A cut-and-cover tunnel was built for the first 700 m. The westernmost 400 m of the double track run in partly very soft clay, in an area surrounded by buildings. Here the depth of the excavation reached 17 m (15 m below the ground water level). The excavation was supported by up to four levels of tie-back anchors installed into bedrock. In total, more than 1000 anchors were installed. The final structure was either founded directly on bedrock or on steel core piles that were drilled into bedrock. The depth to bedrock varied significantly along the alignment from outcrop rock to 40 m. The soft ground above the bedrock consists mostly of clay. A moraine layer with variable thickness was registered above the bedrock and below the very thick clay deposit. The soft clay was characterized as normally consolidated. Undrained shear strength s_u was in the range of 5–15 kPa. The geotechnical parameters of the clay are: tangent modulus M = 5 MPa, Janbu's module number m = 15–22 and consolidation coefficient c_v = 2–10 m^2/year (Braaten et al., 2004).

During the excavation work, considerable drainage to the excavation occurred through or around casings for tie-back anchors and drilled piles. Considerable pore pressure decrease was observed as far as 200–300 m from the excavation (Braaten et al., 2004). Levelling bolts were installed on buildings within 100 m from the excavation and

settlements of up to 14 cm were recorded. Brendbekken et al. (2004) summarise the geotechnical design and Braaten et al. (2004) provide a detailed discussion of this case study including a likely explanation of the observed pore pressure reduction and excavation-induced settlements. A summary of the main parameters used as input for the damage assessment analysis of Jong-Asker case study are summarized in Table 6.

4.3. Jong-Asker results

The maps obtained through the application of the tool are shown in Fig. 8. The impact has been evaluated considering the vertical settlements caused by both short-and long-term settlements and has been classified into 4 classes (see Section 3.2). The houses are categorised considering the maximum vertical settlement of the corner points. Most of the houses (28 out of 29) have a predicted maximum vertical settlement greater than 10 mm (Fig. 9a). The main factors producing impact on the houses are the depth of the excavation, the distance from the excavation and the depth to bedrock. The vulnerability of buildings was evaluated considering four out of five parameters: length and shape (geometrical characteristics), foundation type (structural characteristics) and visual damages (condition). The houses are wooden with shallow foundations. The visual damage varies, essentially, between good and medium. The final vulnerability index does not vary significantly (between medium and high, Fig. 9b), since the houses have the same structural characteristics and similar geometries. The combination of impact and vulnerability is depicted in Fig. 9c, where the houses are coloured in accordance with the estimated damage class (see Section 3.4). Most of the houses (55%) have a predicted level of damage between D0-D2 (Fig. 10a). Respectively 31% and 14% of the houses were predicted to be in damage classes D3 and D4/D5. The damage to houses in these damage classes may vary from minor functional damage to serious structural damages i.e., from doors and windows sticking, to distorted frames, walls bulging, service pipes disrupted and, in extreme cases, beams losing bearing, walls badly leaning, and windows breaking, requiring major repair.

A comparison between the predicted and the back-calculated damage classes was carried out. The differential settlement was calculated for each house, as the maximum among all the corner points, and was used to define damage classes accordingly to the criteria described in Section 4.1. The comparison between predicted and back-calculated damage classes, evaluated from the measured settlements, is provided in Fig. 9d. The predicted buildings with damage classes D3-D4/D5 are overestimated using the proposed method (Fig. 10). A detailed analysis, quantifying the overestimation level is provided in Section 5.

4.4. Project description: Kredittkassen

This excavation in Oslo had a depth of 16 m over an area of around 150 m × 100 m. The excavation was supported by a sheet pile wall installed to bedrock, supported by five levels of tie-back anchors drilled to bedrock. The soil conditions consisted of 1–2 m dry crust clay over normally consolidated soft clay. Beneath 8 m depth, the clay was quick. The depth to bedrock in that area varies from 10 to 30 m. The excavation was performed in an urbanized area in Oslo, surrounded by several old buildings, some of them founded on shallow foundations. Undrained shear strength, s_u, in clay is generally between 15 and 40 kPa. The natural water content is around 30–40%, and soil unit weight is 19 kN/m^3. The groundwater level is at approximately 2–3 m below terrain. The pore pressure measurements showed a pressure distribution with depth somewhat lower than hydrostatic. A summary of the input parameters
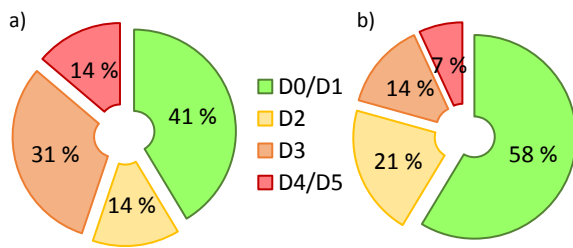
Fig. 10. Percentage of buildings belonging to different damage classes for Jong-Asker case study: (a) Predicted; (b) Back-calculated.

Fig. 12. Percentage of building belonging to different damage classes for *Kredittkassen* case study: (a) Predicted; (b) Back-calculated.

for this case study is provided in Table 6.

Ongoing settlements of 20 mm/year were registered at the time of construction, caused by drainage to existing tunnels in the area that caused a pore water pressure reduction at the bedrock of around 10–35 kPa. The bedrock beneath the sheet pile wall was grouted to a depth of 10–15 m below the bedrock surface. The rock grouting was drilled vertically from the terrain level. Six infiltration wells were used to maintain pore pressure levels during construction. The pore pressure was monitored at bedrock and in the clay with several piezometers.
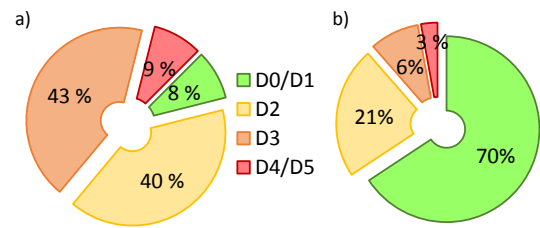
4.5. Kredittkassen results

The results obtained by applying the tool to this case study are shown in Fig. 11. Also, for this case the impact was evaluated considering the vertical settlements as the main deformation parameter (see Section 3.2). The impact analysis alone predicts that 25 out of 33 (76%) buildings are in the highest impact class (I4). The remaining buildings (24%) belong to the second highest class (I3). This is mostly due to the buildings proximity to the excavation, typical of an urban environment, and the large depth to bedrock, up to 35 m (Fig. 11a). Based on the information available, the vulnerability of buildings was evaluated considering three parameters: length and shape (geometrical characteristics), and foundation type (structural characteristics). The vulnerability
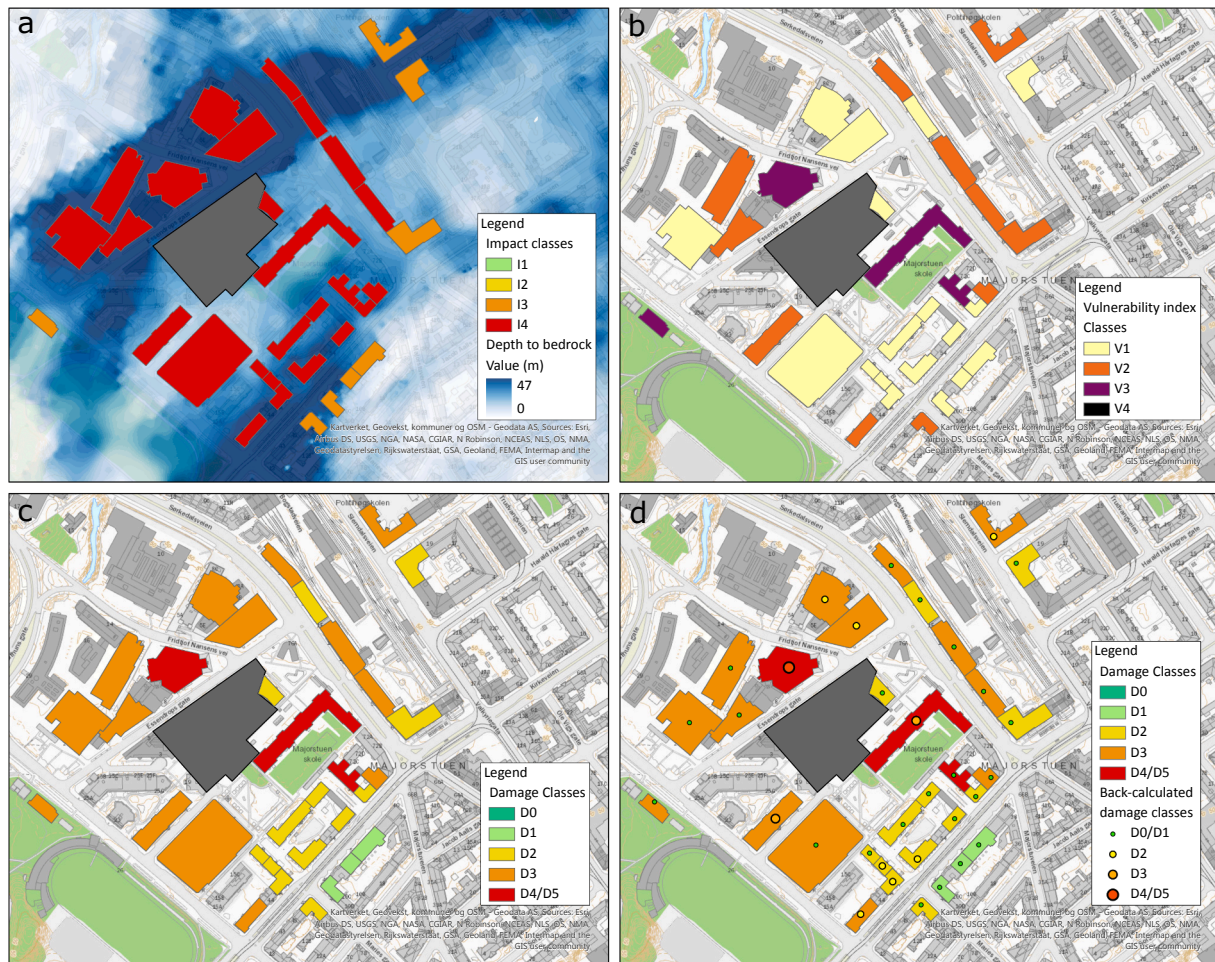

Fig. 11. Maps obtained applying the tool to the *Kredittkassen* case study: (a) Impact classes; (b) Vulnerability classes c. Damage classes; d. Comparison between predicted damage classes and back-calculated ones (dots).
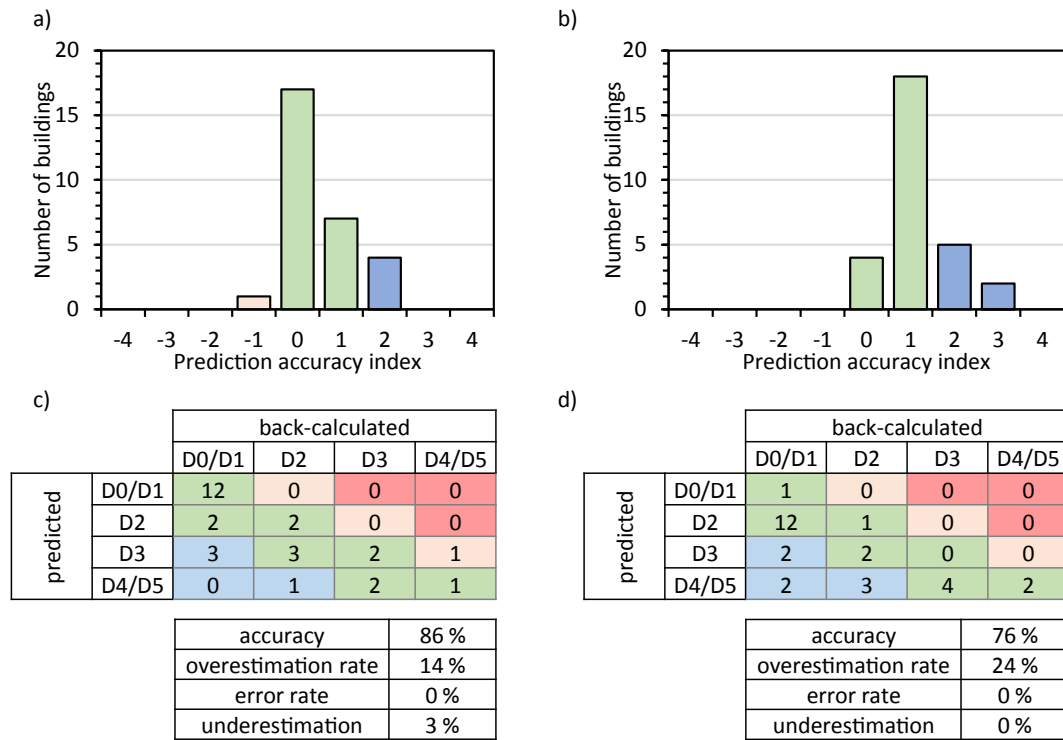
Fig. 13. Jong-Asker case study. The performance analysis has been carried out comparing the damages classes predicted considering the coupled analysis (a, c) and just the impact (b, d). The prediction accuracy index (PAI), as defined by Schuster et al. (2009) (a, b), and the contingency matrix (c, d) have been evaluated.

classes vary from low to high (Fig. 11b). The buildings falling into the high vulnerability class are characterized by having both a shallow foundation and complex geometry. The impact and vulnerability are combined in the matrix (see Section 3.4) to define the final expected damage classes (Fig. 11c). For 48% of the buildings, damage classes between D0-D2 were predicted (Fig. 12a). The remaining buildings have a damage class of D3 (43%) and D4/D5 (9%).

A comparison between the predicted and the measured damage classes is provided in Figs. 11d and 12. The damage classes for the measured settlements were again back-calculated considering the fragility curves from Peduto et al. (2019). The differential settlement was calculated for each building and was used to define damage classes accordingly to the criteria described in Section 4.1. In Fig. 11d the coloured dots represent the damage classes evaluated considering the measured settlements. Also, for this case study, an overestimation of damage classes D3-D4/D5 is observed using the proposed method. The predicted exposed buildings in damage classes D4/D5 are 9% against the 3% calculated considering the measured settlements. There is a high percentage of buildings predicted by the tool with a damage class D3 (43%). This seems to be a quite high overestimation. A detailed analysis is carried out in Section 5 to better understand the reasons for this finding.

5. Discussion

The previous section described the results obtained by applying the tool to two case studies. The comparison between predicted and back-calculated damage classes showed that the tool tends to overestimate the number of buildings in damage classes D3-D4/5. This agrees with the rationale of avoiding underestimation of potential damage to

Table 7
Jong-Asker case study. Performance indicators considering the coupled analysis and just the impact.

	Impact and vulnerability	Impact
accuracy	86%	76%
overestimation rate	14%	24%
error rate	0%	0%
underestimation	3%	0%

neighbouring buildings and unexpected economic losses. On the other hand, one would want to avoid excessive overestimations and to focus attention and resources on buildings that are most susceptible to damage. A detailed analysis of the method performance is described in the following. A quantification of the accuracy, overestimation, underestimation and error rates is provided for both case studies. Moreover, a detailed comparison between predicted and back-calculated damage classes, considering just the impact (no vulnerability) and the coupled analysis (impact and vulnerability), has been carried out and is presented in the following.

The performance analysis was carried out by evaluating the prediction accuracy index (PAI), as defined by Schuster et al. (2009), and evaluating performance indicators of a contingency table (Calvello and Piciullo, 2016; Piciullo et al., 2020). The PAI is calculated for each building by taking the difference between the predicted and the back-calculated damage classes. The index indicates the number of classes a building has been under- or overestimated. The value is positive for overestimation and negative for underestimation. Figs. 13a and 14a show the PAI respectively for the Jong-Asker and Kredittkassen case studies. The results for the latter case study show a higher number of
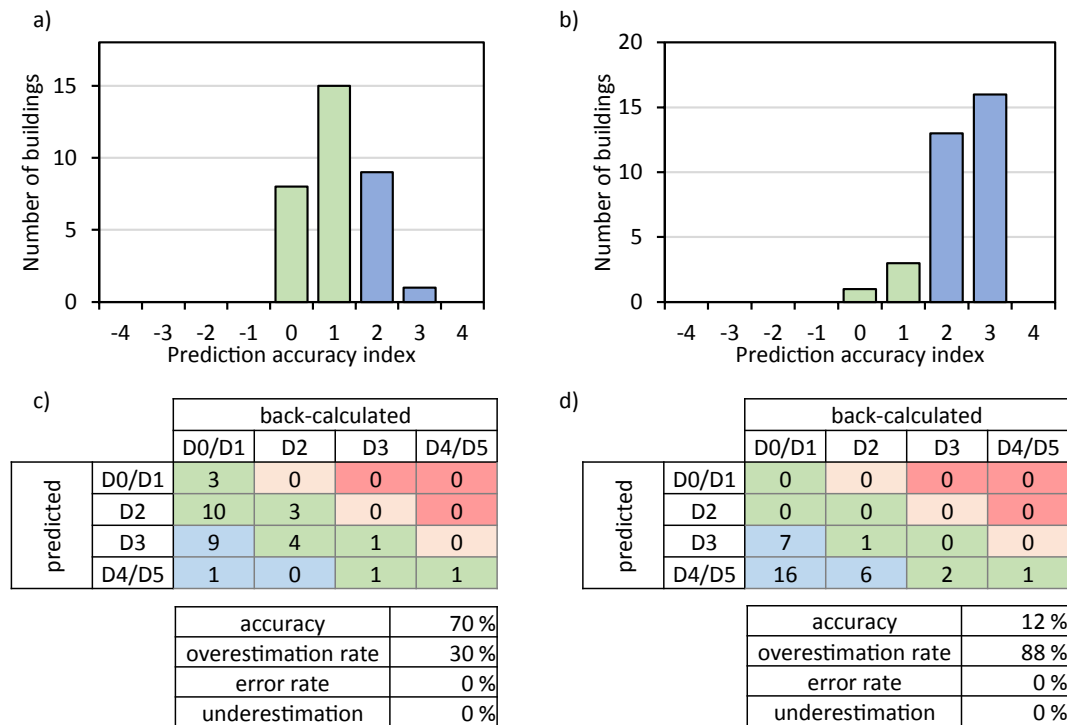
a)

b)

c)

		back-calculated			
		D0/D1	D2	D3	D4/D5
predicted	D0/D1	3	0	0	0
	D2	10	3	0	0
	D3	9	4	1	0
	D4/D5	1	0	1	1

accuracy	70 %
overestimation rate	30 %
error rate	0 %
underestimation	0 %

d)

		back-calculated			
		D0/D1	D2	D3	D4/D5
predicted	D0/D1	0	0	0	0
	D2	0	0	0	0
	D3	7	1	0	0
	D4/D5	16	6	2	1

accuracy	12 %
overestimation rate	88 %
error rate	0 %
underestimation	0 %

Fig. 14. *Kredittkassen* case study. The performance analysis has been carried out comparing the damages classes predicted considering the coupled analysis (a, c) and just the impact (b, d). The prediction accuracy index (PAI), as defined by Schuster et al. (2009) (a, b), and the contingency matrix (c, d) have been evaluated.

Table 8
Kredittkassen case study. Performance indicators considering the coupled analysis and just the impact.

	Impact and vulnerability	Impact
accuracy	70%	12%
overestimation rate	30%	88%
error rate	0%	0%
underestimation	0%	0%

overestimated buildings. The contingency tables (or contingency matrices) and indicator values are respectively provided in Fig. 13c and Table 7 for the Jong-Asker case study and in Fig. 14c and Table 8 for Kredittkassen. The Jong-Asker case study has a high accuracy (86%) with an overestimation rate of 14%. Four out of 29 buildings were overestimated by two damage classes (Fig. 13a, c). The underestimation rate is 3% because one building was underestimated by one damage class (D3 instead of D4/D5). The Kredittkassen results show a lower accuracy (70%) and a higher overestimation rate (30%) compared to Jong-Asker. Nine out of 33 buildings were overestimated by two damage classes and one building by three classes (Fig. 14a, c). The error rate and the underestimation rate are both 0% (Fig. 14c). The two case studies show a relatively high accuracy, and a low or null underestimation rate. It is important to underline that none of the case studies showed errors (defined as underestimation of 2 or more damage classes). However, Kredittkassen showed a quite high overestimation rate (30%): D3 was predicted for nine buildings instead of D0/D1 (Fig. 14a). This result could be refined if more information about the building type of structure were gathered. In this way, the vulnerability model could be improved, probably leading to lower damage classes for some of the buildings. It is also important to mention that the long-term settlements were calculated considering full primary consolidation and this also may lead to an overestimation of the impact classes for buildings. One option to resolve this issue is to implement the U-T curve of Terzaghi and to evaluate the degree of consolidation at a time step that represents the period the excavation remained open. Moreover, the maximum vertical displacement of a building is used as the metric to define the buildings impact classes (see Section 3). This displacement parameter cannot be related to building deformations (i.e. strains) and thus likely overestimates the damage class. Further improvement of the proposed method is also envisioned when the predictions can be directly related to observed damage based on building inspections.

To evaluate the importance of considering the vulnerability of buildings in the damage assessment, the predicted damage classes obtained considering just the impact model were compared with the coupled analysis that considers both impact and vulnerability. Figs. 13 and 14 respectively show the detailed results of the performance analysis for Jong-Asker and Kredittkassen case studies. Tables 7 and 8 summarize the indicators values. One can observe that the model considering just the impact has lower accuracy and higher overestimation rate for both case studies. For Kredittkassen, the overestimation rate considering solely the impact is very high (88%), since 29 out of 33 buildings are overpredicted of more than two damage classes (Fig. 14d). This is in line with the discussion above on the calculation of the long-term settlements and impact classes.

6. Conclusions

An original methodology for the assessment of building damage due to excavation-induced displacements was described. Both the impact (i. e. short- and long-term displacements caused by the excavation) and the vulnerability of the neighbouring buildings are considered in the GIBV damage assessment method. Considering the long-term settlement and vulnerability of the buildings in the damage assessment is an innovative aspect of the methodology. The comparative analyses carried out for two case studies showed that coupling the impact analysis with vulnerability assessment increases the accuracy of the damage class predictions. A model that is exclusively based on the impact evaluation, which applies the greenfield displacements to the buildings and neglects the soil-

structure interaction, will lead to overestimation of the buildings damage classes. On the other hand, in excavations producing high porewater pressure reduction, neglecting the long-term consolidation processes will lead to an underestimation of the impact.

The GIBV method was implemented in ArcGIS software using Python scripts, providing a user-friendly tool for preliminary evaluation of buildings prone to damages due to excavation-induced displacements. The GIS environment enables conducting a rapid assessment for a considerable number of buildings, which is particularly crucial for pre-construction damage assessment of infrastructure projects in urban settings. The application of the tool was demonstrated for two excavations in different urban contexts. The performance analysis showed relatively good accuracy for both case studies. The tool is modular, long-term displacements and vulnerability analyses can be neglected for lack of information, or if not relevant.

The empirical curves currently implemented into the impact analysis are a simple way to estimate the expected settlements as a function of geometric distance from an excavation. On the other hand, these curves are representative of a specific type of excavation and soil (i.e., Norwegian clay). The short-term analysis considers empirical curves representative of internally braced excavations supported by sheet pile walls, with different factor of safety and wall depths. The long-term analysis is based on measured observations of pore water pressure reduction in different excavation projects in Norway. Both for the short-term and long-term analysis, the empirical curves can be adjusted/substitued to represent other ground conditions. The vulnerability assessment is based on six parameters. The weights assigned to them can be changed accordingly to the reliability of the information at hand.

Currently, the GIBV method is based on the computation of maximum settlements and slope values respectively for the corner points and walls of buildings. The methodology can be further developed implementing new relations for different retaining structures and type of soils in the impact analysis, considering a more quantitative soil-structure interaction, evaluating settlements at different degrees of consolidations and quantifying the uncertainties on the geotechnical parameters. Moreover, a natural progression of this work would be to obtain more direct data on building damage caused by excavation works. Such future data could be used to better compare predicted and observed building damage and could be used for refining the calibration of the GIBV method. Deformation parameters other than the maximum settlement and slope (i.e., deflection ratio, the angular distortion and the horizontal strain) are currently under consideration for damage assessment.

CRediT authorship contribution statement

Luca Piciullo: Conceptualization, Methodology, Validation, Writing - original draft, Visualization, Formal analysis, Investigation. **Stefan Ritter:** Conceptualization, Methodology, Validation, Writing - review & editing. **Asgeir Olaf Kydland Lysdahl:** Software, Formal analysis. **Jenny Langford:** Supervision, Project administration, Writing - review & editing. **Farrokh Nadim:** Supervision, Writing - review & editing.

Declaration of Competing Interest

The authors declare that they have no known competing financial interests or personal relationships that could have appeared to influence the work reported in this paper.

References

Abdel-Rahman, A.H., 1993. Numerical modeling of concrete diaphragm walls. M. Sc. Thesis. Ain Shams University, Cairo, Egypt.

Andresen, L., Jostad, H. P., 2004. Janbu's Modulus Concept vs. Plaxis Soft Soil Model. NGM 2004 - XIV Nordic Geotechnical Meeting. https://doi.org/10.13140/RG.2.1.2397.8729.

Aye, Z.Z., Karki, D., Schulz, C., 2006. Ground Movement Prediction and Building Damage Risk-Assessment for the Deep Excavations and Tunneling Works in Bangkok Subsoil. International Symposium on Underground Excavation and Tunnelling, Urban Tunnel Construction for Protection of Environment Sponsored by International Tunnelling Association (ITA/AITES), 2-4 February 2006, Bangkok, Thailand, pp. 281–297.

Bentler, D.J., 1998. Finite Element Analysis of Deep Excavations. PhD thesis. Virginia Polytechnic Institute and State University.

Bhattacharya, S., Singh, M.M., 1984. Proposed criteria for subsidence damage to buildings. Rock mechanics in productivity and protection. American Rock Mechanics Association the 25th U.S. Symposium on Rock Mechanics (USRMS), 25-27 June, Evanston, Illinois, pp. 747–755.

Boscardin, M.D., Cording, E.J., 1989. Building response to excavation induced settlement. J. Geotech. Eng. ASCE 115 (1), 1–21. https://doi.org/10.1061/(ASCE)0733-9410(1989)115:1(1).

Bowles, J.E., 1988. Foundation Analysis and Design. McGraw-Hill, Inc., New York.

Braaten, A., Baardvik, G., Vik, A., Brendbekken, G., 2004. Observed effects on the pore pressure caused by extensive foundation work and deep excavations in clay. Proceedings of the Nordic Geotechnical Conference, Ystad, Sweden, H119-H132 (in Norwegian).

Brendbekken, G., Baardvik, G., Braaten, A., Vik, A., 2004. Geotechnical design of deep excavation in soft quick clay with instrumentation of sheet pile wall and struts to control its functionality. In: Proceedings of the Nordic Geotechnical Conference, Ystad, Sweden: A85-A203 (in Norwegian).

Broere, W., 2016. Urban underground space: solving the problems of today's cities. Tunn. Undergr. Space Technol. 55, 245–248. https://doi.org/10.1016/j.tust.2015.11.012.

Burland, J.B., 1995. Assessment of damage to buildings due to tunneling and excavation. In: Invited Special Lecture to IS-Tokyo 1995: Proceedings of 1st International Conference on Earthquake and Geotechnical Engineering, Tokyo, pp. 1198–1201.

Burland, J.B., Broms, B., DeMello, V.F.B., 1977. Behaviour of foundations and structures: state of the art report. In: Proceedings of 9th International Conference on Soil Mechanic and Foundation Engineering, vol. 3, Balkema, Rotterdam, pp. 495–546.

Burland, J.B., Wroth, C.P., 1974. Settlement of buildings and associated damage. In: Proceedings of Conference on Settlement of Structures, Cambridge, pp. 611–654.

Calvello, M., Piciullo, L., 2016. Assessing the performance of regional landslide early warning models: the EDuMaP method. Nat. Hazards Earth Syst. Sci. https://doi.org/10.5194/nhess-16-103-2016, 2016.

Caspe, M.S., 1966. Surface settlement adjacent to braced open cuts. J. Soil Mech. Found. Div., ASCE 92 (SM4), 51–59.

Castaldo, P., Calvello, M., Palazzo, B., 2013. Probabilistic analysis of excavation-induced damages to existing structures. Comput. Geotech. 53, 17–30. https://doi.org/10.1016/j.compgeo.2013.04.008.

Chiriotti E., Marchionni. V. Grasso, P., 2000. Porto Light Metro System, Lines C, S and J. Interpretation of the Results of the Building Condition Survey and Preliminary Assessment of Risk. Methodology for Assessing the Tunnelling Induced Risks on Buildings along the Tunnel Alignment. Normetro – Transmetro, Internal technical report (in Italian and Portuguese).

Chiriotti, E., Grasso, P., 2001. Porto Light Metro System, Lines C, S and J. Compendium to the Methodology Report on Building Risk Assessment Related to Tunnel Construction. Normetro – Transmetro, Internal technical report (in English and Portuguese).

Clarke, J., Hannigan, L., 2009. A three-stage assessment process to predict risk levels due to subsurface construction. In: Proceedings of 34th Annual Conference on Deep Foundations, Kansas City, Publication no. 89 (AM-2009).

Clarke, J., Laefer, D.F., 2014. Evaluation of risk assessment procedures for buildings adjacent to tunnelling works. Tunn. Undergr. Sp. Tech. 40 (2014), 333–342. https://doi.org/10.1016/j.tust.2013.10.014.

Clough, G.W., O'Rourke, T.D., 1990. Construction induced movements of in situ walls. In: Lambe, P.C., Hansen, L.A. (Eds.), Proc. ASCE Design Performance Earth Retaining Struct., Ithaca, NY, June 18–21, pp. 439–470.

Dzegniuk, B., Hejmanowski, R., Sroka, A., 1997. Evaluation of the damage hazard tobuilding objects on the mining areas considering the deformation course in time. In: Proceedings of Xth International Congress of the International Society for Mine Surveying. https://doi.org/10.13140/2.1.3356.3520.

El-Nahhas, F., Morsy, M.M. 2002. Comparison of the measured and computed performance of propped diaphragm retaining wall in Egypt. Proc. of the Int. Symposium on Numerical Models in Geomechanics, Rome, Italy, pp. 579-586.

El-Sayed, S.M., Abdel-Rahman, A.H., 2002. Spatial stress-deformation analysis for installation of a diaphragm wall. Faculty of Engineering Scientific Bulletin, Ain Shams University, vol. 37, No. 3, Cairo, Egypt.

Eriksson, I., Adamou, S., Sæther, M. M., Bekkhus, R., 2014. Oslo kommune. Plan- og bygningsetaten. Prosjekt for økt kunnskap om undergrunn i Oslo. Delprosjekt grunnvann. Utvikling av metode for kartlegging av områder med bevaringsverdig bebyggelse som er sensitive for endringer i grunnvannsforhold. Datert 2014.12.19.

Ferreira, T.M., Vicente, R., Mendes da Silva, J.A.R., Varum, H., Costa, A., 2013. Seismic vulnerability assessment of historical urban centres: case study of the old city centre in Seixal, Portugal. B. Earthq. Eng. 11 (5), 1753–1773. https://doi.org/10.1007/s10518-013-9447-2.

Ferreira, T.M., Vicente, R.S., Varum, H., 2014. Seismic vulnerability assessment of masonry facade walls: development, application and validation of a new scoring method. Struc. Eng. Mech. 50 (4), 541–561. https://doi.org/10.12989/sem.2014.50.4.541.

Finno, R.J., Harahap, I.S., 1991. Finite element analysis of HDR-4 excavation. J. Geotech. Geoenviron. 117 (10), 1590–1609. https://doi.org/10.1061/(ASCE)0733-9410(1991)117:10(1590).

Giardina, G., Hendriks, M.A.N., Rots, J.G., 2010. Numerical analysis of tunnelling effects on masonry buildings: the influence of tunnel location on damage assessment. In: Gu, X., Song, X. (Eds.), Advanced Materials Research, Shanghai, vol. 133, pp. 289–294. https://doi.org/10.4028/www.scientific.net/AMR.133-134.289.

Giardina, G., Floria, V., Hendriks, M., Rots, J., 2012. Vulnerability assessment of buildings subject to tunnel-induced settlements: the influence of orientation and position of the building. In: Phienwej, N., Boonyatee, T. (Eds.), Proceedings of the World Tunnelling Congress, Bangkok. ISBN, 9789747197785.

Giardina, G., Hendriks, M.A.N., Rots, J.G., 2009. Assessment of the settlement vulnerability of masonry buildings. In: 1st WTA International PhD Symposium – Buildings Materials and Building Technology for preservation of the Built Heritage, Leuven, Belgium.

GNDT, 1993. Rischio Sismico Di Edifici Pubblici, Parte I: Aspetti Metodologici, Proceedings of CNR-Gruppo Nazionale per la Difesa dai Terremoti, Roma, Italy (1993) (in Italian).

Gokhale, D.V., Kullback, Solomon, 1978. The Information in Contingency Tables. Marcel Dekker. ISBN 0-824-76698-9.

Goldberg, D.T., Jaworski, W.E., Gordon, M.D., 1976. Lateral support systems and underpinning. Report FHWA-RD-75-128, Federal Highway Administration, Washington D.C., 1, 312.

Grünthal, G., 1998. European Macroseismic Scale 1998 (EMS-98) European Seismological Commission, Subcommission on Engineering Seismology, 15. Brussels: Cahiers du Centre Européen de Géodynamique et de Séismologie: Working Group Macroseismic Scales. ISBN No2-87977-008-4.

Guglielmetti, V., Grasso, P., Mahtab, A., Xu, S., 2008. Mechanized Tunnelling in Urban Areas: Design Methodology and Construction Control. Taylor & Francis, London. https://doi.org/10.1201/9780203938515.

Hashash, Y.M.A., Whittle, A.J., 1996. Ground movement prediction for deep excavations in soft clay. J. Geotech. Eng. 122 (6), 474–486. https://doi.org/10.1061/(ASCE)0733-9410(1996)122:6(474).

Hashash, Y.M.A., Whittle, A.J., 2002. Mechanism of load transfer and arching for braced excavations in clay. J. Geotech. Geoenviron. 128 (3), 187–197. https://doi.org/10.1061/(ASCE)1090-0241(2002)128:3(187).

Hsieh, P.-G., Ou, C.-Y., 1998. Shape of ground surface settlement profiles caused by excavation. Can. Geotech. J. 35 (6), 1004–1017. https://doi.org/10.1139/t98-056.

Janbu, N., 1970. Grunnlag i geoteknikk. Trondheim: Tapir forlag Brinkgreve, R.B.J. 2002. PLAXIS 2D – version 8. A.A. Balkema Publishers. The Netherlands.

Jennings, J.E., Kerrich, J.E., 1962. The heaving of buildings and the associated economic consequences, with particular reference to the Orange Free State goldfields. The Civ. Engr. in South Africa 5 (5), 122.

Jollifee, I.T., Stephenson, D.B., 2003. Forecast verification. A Practitioner's Guide in Atmospheric Science. John Wiley, Chichester, p. 240.

Karlsrud, K., Andresen, L., 2005. Loads on braced excavations in soft clay. ASCE Int. J. Geomech. 5 (2), 107–114. ISSN 1532-3641.

Karlsrud, K., 1997. Some aspects of design and construction of deep supported excavation, Discussion leader's contribution. In: Proc. 14th Int. Conf. on Soil Mech. Found. Eng. Hamburg. 4, pp. 2315–2320.

Konstantakos, D.C., 2008. Online database of deep excavation performance and prediction. In: 6th International Conference on Case Histories and Geotechnical Engineering. Arlington, paper 5.16 (1-12).

Kung, G.T.C., 2003. Surface settlement induced by excavation with consideration of small strain behavior of Taipei silty clay. PhD Dissertation. Department of Construction Engineering, National Taiwan University of Science and Technology, Taipei, Taiwan. Kwiatek, 1998.

Kung, G.T.C., Hsiao, E.C.L., Juang, C.H., 2007. Evaluation of a simplified small strain soil model for estimation of excavation-induced movements. Can. Geotech. J. 44, 726–736. ISSN:1208-6010.

Kung, G.T.C., Ou, C.Y., Juang, C.H., 2009. Modeling small-strain behaviour of Taipei clays for finite element analysis of braced excavations. Comput. Geotech. 36 (1–2), 304–319.

Lande, E.-J., Karlsrud, K., Langford, J., Nordal, S., 2020. Effects of drilling for tie-back anchors on surrounding ground – results from field tests. Int J Geotech Geoenviron Eng.

Langford, J., Karlsrud, K., Lande, E.J., Eknes, A.Ø., Engen, A., 2015. Causes of unexpectedly large settlements induced by deep excavations in soft clay. In: Winter, M.G., Smith, D.M., Eldred, P.J.L., Toll, D.G. (Eds.), Proceedings of the XVI ECSMGE Geotechnical Engineering for Infrastructure and Development. ICE publishing, pp. 1115–1120.

Langford, J., Baardvik, G., 2016a. Pore pressure reduction and settlements induced by deep supported excavations in soft clay. In: Proceedings of the 17th Nordic Geotechnical Meeting, NGM 2016 Reykjavik. ISBN: 978-9935-24-002-6.

Langford, J., Karlsrud, K., Lande, E.J., Baardvik, G., Engen, A., 2016. BegrensSkade – Limitation of damage caused by groundworks. In: Grundläggningsdagen GD2016. Stock-holm, Sweden.

Long, M., 2001. Database for retaining wall and ground movements due to deep excavations. J. Geotech. Environ. 127 (3), 203–224. ISSN: 1090–0241.

MacLeod, I.A., Littlejohn, G.S., 1974. Discussion of session 5. In: Proc, Conf. on Settlement of Structures, Pentech Press, London, England, pp. 792–795.

Maio, R., Ferreira, T.M., Vicente, R., Estêvão, J., 2016. Seismic vulnerability assessment of historical urban centres: case study of the old city centre of Faro, Portugal. J. R. Res. 19 (5), 551–580. https://doi.org/10.1080/13669877.2014.988285.

Mair, R.J., Taylor, R.N., Burland, J.B., 1996. Prediction of Ground Movements and Assessment of Risk of Building Damage. Geotechnical Aspects of Underground Construction in Soft Ground, Balkema, Rotterdam, pp. 712–718.

Mana, A.I., Clough, G.W., 1981. Prediction of movements for braced cuts in clay. J. Geotech. Eng., Am. Soc. Civil Eng. 107, 759–777.

Moormann, C., Moormann, H.R., 2002. Study of wall and ground movements due to deep excavation in soft soil based on worldwide experiences. Geotechnical Aspects of Underground Construction in Soft Ground, Toulouse, Spécifique, Lyon, pp. 477–482. ISBN 2-9510416-3-2.

National Coal Board, 1975. Subsidence engineer's handbook. National Coal Board Productions Department, London.

Ng, C.W.W., 1992. An evaluation of soil-structure interaction associated with a multi-propped excavation. Ph.D. Thesis. University of Bristol, UK.

Ng, C.W.W., Yan, W.M., 1999. Three-dimensional modelling of a diaphragm wall construction sequence. Geotechnique 49 (6), 825–834. https://doi.org/10.1680/geot.1999.49.6.825.

O'Rourke, T.D., 1981. Ground movements caused by braced excavations. J. Geotech. Eng., Am. Soc. Civil Eng 107, 1159–1178.

O'Rourke, T.D., 1993. Base Stability and Ground Movement Prediction for Excavations in Soft Clay. Retaining Structures. Thomas Telford, London, pp. 131–139.

Ou, C.Y., Shiau, B.Y., Wang, I.W., 2000. Three-dimensional deformation behavior of the Taipei National Enterprise Center (TNEC) excavation case history. Can. Geotech. J. 37 (2), 438–448. https://doi.org/10.1139/t00-018.

Ou, C.Y., Hsieh, P.G., Chiou, D.C., 1993. Characteristics of ground surface settlement during excavation. Can. Geotech. J. 30 (5), 758–767. https://doi.org/10.1139/t93-068.

Peck, P.B., 1969. Deep excavations and tunneling in soft ground. In: Proceedings of 7th International Conf. on Soil Mechanics and Foundation Engineering, Mexico City, 3, pp. 225–290.

Peduto, D., Korff, M., Nicodemo, G., Marchese, A., Ferlisi, S., 2019. Empirical fragility curves for settlement-affected buildings: Analysis of different intensity parameters for seven hundred masonry buildings in The Netherlands. Soils Found. 59, 380–397. https://doi.org/10.1016/j.sandf.2018.12.009.

Piciullo, L., Tiranti, D., Pecoraro, G., Cepeda, J.M., Calvello, M., 2020. Standards for the performance assessment of territorial landslide early warning systems. Landslides 2020. https://doi.org/10.1007/s10346-020-01486-4.

Poh, T.Y., Goh, A.T.C., Wong, I.H., 2001. Ground movements associated with wall construction: case Histories. J. Geotech. Geoenvir., ASCE 127 (12), 1061–1069. https://doi.org/10.1061/(ASCE)1090-0241(2001)127:12(1061).

Polsby, D., Popper, R., 1991. The Third Criterion: Compactness as a procedural safeguard against partisan gerrymandering. Yale Law J. 9 (2), 301–353. https://doi.org/10.2139/ssrn.2936284.

Rankin, W.J., 1988. Ground movements resulting from urban tunnelling: predictions an effect. Geological Society, London, Eng. Geo. Sp. 5, 79–92. https://doi.org/10.1144/GSL.ENG.1988.005.01.06.

Saeidi, A., Deck, O., Verdel, T., 2012. Development of building vulnerability functions in subsidence regions from analytical methods. Geotechnique 62 (2), 107–120. https://doi.org/10.1680/geot.9.P.028.

Schuster, M.J., Kung, G.T.C., Juang, C.H., Hashash, Y.M.A., 2009. Simplified model for evaluating damage potential of buildings adjacent to a braced excavation. J. Geotech. Geoenviron. 135 (12), 1823–1835. https://doi.org/10.1061/(ASCE)GT.1943-5606.0000161.

Son, M., Cording, E.J., 2005. Estimation of building damage due to excavation-induced ground movements. J. Geotech. Geoenviron. 131 (2), 162–177. https://doi.org/10.1061/(ASCE)1090-0241(2005)131:2(162).

Vicente, R.S., Parodi, S., Lagomarsino, S., Varum, H., Mendes da Silva, J.A.R., 2011. Seismic vulnerability and risk assessment: case study of the Historic City Centre of Coimbra, Portugal. B. Earthq. Eng. 9 (4), 1067–1096. https://doi.org/10.1007/s10518-010-9233-3.

Whittle, A.J., Hashash, Y.M.A., Whitman, R.V., 1993. Analysis of deep excavation in Boston. J. Geotech. Eng. 119 (1), 69–90. https://doi.org/10.1061/(ASCE)0733-9410(1993)119:1(69).

Yu, Z., Karmis, M., Jarosz, A., Haycocks, C., 1988. Development of damage criteria for buildings affected by mining subsidence. In: 6th Annual Workshop Generic Mineral Technology Center Mine System Design And Ground Control, pp. 83–92.